Available online at www.sciencedirect.com

ScienceDirect

Procedia Engineering 102 (2015) 831 – 840

Procedia Engineering

www.elsevier.com/locate/procedia

The 7th World Congress on Particle Technology (WCPT7)

Deposition and wear of deposits in swirl spray driers: The equilibrium exchange rate and the wall-borne residence time.

Víctor Francia[a,b,*], Luis Martín[b], Andrew E. Bayly[b], Mark J.H. Simmons[a]

[a]*School of Chemical Engineering, University of Birmingham, Birmingham, B15 2TT, United Kingdom*
[b]*Procter & Gamble R &D, Newcastle Innovation Centre, Newcastle upon Tyne, United Kingdom*

Abstract

Wall deposits are omnipresent in many particle technology operations, such as spray drying and granulation processes. Their impact has been long recognized and is typically considered detrimental to the process performance. Counter-current spray drying units, such as those used in the manufacture of detergents, make use of strong swirling flows which leads to substantial multi-layered deposits at the walls. However their relation to the rest of the process has never been studied in detail. The work presented here discusses the generation of the structure at the walls and how it interacts with the air-borne population of particles. A tracer experiment is outlined that permits one to track the release of material from the deposits and differentiate the origin of aggregates in the product, as being generated either by the atomization or through the erosion of deposits. Monitoring of the wall and analysis of the release rate of the tracer has permitted identification of a dynamic equilibrium between the rates of deposition and re-entrainment, and quantification of the exchange rate above 12-20% of the full production. The age of the re-entrained material, indicative of the time the granules remain resident at the wall, appears much higher than expected for an air-borne trajectory. Such observations suggests that the description of the spray drying process exclusively in terms of the air-borne condition of particles is incomplete, at least in relation to the manufacture of detergents in swirl assisted systems. Focus should be paid to the wall-borne condition of the product, for it is seen to govern the generation of large granule sizes and dominate the residence time and drying kinetics of a significant part of the product.

Selection and peer-review under responsibility of Chinese Society of Particuology, Institute of Process Engineering, Chinese Academy of Sciences (CAS)

Keywords: deposition; re-suspension; re-entrainment; turbulent swirling flow; spray drying; multi-layer;

* Corresponding author.
E-mail address: v.francia.chemeng@gmail.com / VXF935@bham.ac.uk

Selection and peer-review under responsibility of Chinese Society of Particuology, Institute of Process Engineering, Chinese Academy of Sciences (CAS)
doi:10.1016/j.proeng.2015.01.200

1. Introduction.

In a particle technology context, the occurrence of fouling and its interaction with the rest of the process is often not well understood, and rather viewed as an operational matter and not an integral part of the process. Beyond applications such as spray drying or agglomeration, such dynamics occurs in many other fields where particulate, colloidal or biological fouling is often recognized as critical factor and studied in depth. Among the most relevant examples are nuclear engineering, combustion, heat exchange devices, biomedical applications or the petro-chemical industry, where most of the work in deposition and re-entrainment focuses. As a result, the numerical description of fouling and the available experimental works seek the study of interaction between turbulence and deposition, critical in non-inertial or intermediate regimes [1]. As detailed by Henry *et al.* in their review of colloidal fouling [2], most systems deal with mono-layers and evaluation of the particle-surface forces dominating smaller particle size ranges (e.g. Van der Waals or electrostatics) and, in addition, associate re-entrainment purely with the action of disruptive stresses of aerodynamic origin. An important exception to this general trend is the ample body of research in relation to shedding or detachment of large pieces of ash deposits in burners, caused by gravity [3, 4].

In many applications in particle technology it is common to deal with a very wide particle size range, from several microns to several millimeters, thus inertia effects become more important to deposition. Moreover, the use of liquid binders is common and particles often modify their mechanical properties or cohesive strength during processing, such as in melting or drying operations. In these circumstances the situation becomes more complex, particle-particle and particle-surface forces include those of capillary origin and the contact mechanics increase in complexity [5, 6]. The study of particle interactions in spray drying has so far been limited to investigate particle-particle collisions in an air-borne state [7, 8, 9] but the role of the deposits at the walls has not yet been addressed in detail. These would require to include analysis of the multi-layer microstructure of the deposits, and how it interacts with the air-borne particles, growing by deposition or breaking by the re-entrainment of clusters. Nonetheless, extensive work has been carried out to characterized deposition in co-current spray driers, where it can lead to significant operational issues. The work of Ozmen and Langrish summarize the three main issues: [10]: 1- product degradation and safety and quality concerns, 2- a detriment in the yield and the process efficiency and 3- maintenance costs. Many evidences of deposition are available in the food industry [11], where significant efforts have been made to optimize the yield [12, 13, 14]. More recently this has lead to emphasis in the role of particle impacts and deposits re-suspension [15]. In a counter-current spray dryer deposition if far greater than the co-current case due to the process geometry, a higher droplet/particle concentration and, in the case swirl assisted units, by frequent particle contact with the walls. This phenomenon has been always acknowledged [16] in counter-current spray drying of detergents but only recently visualized through PIV techniques [17]. Its impact on particle growth, drying or residence time however was never quantified. It is an accepted fact that detergents contain an unknown proportion of particles that result from re-entrainment of deposits which is simply blended into the rest of the powder. In this work, such a population has been identified by means of a tracer experiment. A more detailed and full description including the analysis of the granules morphology and the re-entrainment mechanics will be available in a separate publication [18]. This paper provides a general outline of the methodology and introduces to spray drying the concept of 1- the exchange rate due to a dynamic equilibrium between deposition rate and re-entrainment rate at the walls, and 2- the wall-borne residence time of the product.

2. Experimental methodology.

2.1 Operation of counter-current spray drying towers.

Fig. 1 depicts the industrial counter-current spray drying tower used in this work including the tracer injection designed for the study of the wall dynamics. The hot air rises in the cylindrical body of the tower after injection into the bottom conical section by a series of symmetrical inlets. Their orientation provides an initial angular momentum to the flow, which causes the air to swirl. The vortex generated rises in the unit and converges inwards, exiting the tower by a centrally located conduit at its top, named the vortex finder, after which the air passes through a cyclones where any elutriated powder is removed.

A standard detergent formulation is produced in a batch mixer by the addition of surfactant/s, polymer/s and inorganic salts, up to overall solids content between 30-60 % in mass. Transition to a continuous process is achieved via a holding tank, after which the mix is pumped through a hammer mill, brought to high pressure and conducted to a single pressure hollow cone nozzle placed inside the unit, at a central location aligned with the cylinder axis and facing downwards. After atomization, the droplets/particles acquire the swirling motion from the air vortex, and as governed by their size and density begin to flow downwards and dry, leaving the unit in the form of particulate product. Small particle size fractions, typically below 10% in mass, are elutriated and separated in cyclones. Combination of a high centrifugal inertia with the high moisture content of semi-dried particles results in a high deposition level. Most of the product concentrates nearby the wall, and the trajectories of droplets/particles contain multiple wall impacts before they can reach the exit. As drying progresses, the droplet properties and consequently their impact behavior changes. Drier particles typically rebound or cause erosion of deposits. As they dry, particle impacts become more elastic and thus inefficient, not resulting in aggregation or deposition but in rebound or the erosion of material from the multi-layer. Otherwise, at an initial stage of drying, wet wetter particles can deform upon the impact to the wall and deposit. The area where most atomized droplets impact for the first time is therefore where the deposits are thickest [17]. This position roughly corresponds to a projection of the spray cones to the wall where the expected impact rate is higher, and the spayed droplets reach the wall at a higher momentum and water content. In addition to the wall inspection throughout the rest of the cylinder, this particular area was studied independently. A dismountable plate was designed to be flushed with the inner wall and put in place at that section. At intervals during the execution of the experiments it was extracted, weighted and placed back in position, monitoring directly the net deposition rate of material. Measurement of particle size and separation into size fractions was obtained by sieving, making use of the Taylor series. Sampling was performed at the exit of the tower belt in Fig. 1 by collecting the entire exit stream and subsequently sampling it down for analysis.

A tracer injection system for an aqueous solution of the tracer was installed at the low pressure line. A fluorescent visible dye, Sanolin Rhodamine B02, water soluble and proven to sustain the temperature range, was used. The injection rate was controlled to obtain 100 ppm in the final particulate product. The tracer content in the powder samples was determined by the use of a UV/Visible spectrophotometer (Shimadzu UV-2401PC) at the maximum absorbance wave length 565 nm. In order to be able to execute a sudden change between the atomization of slurry or pure water into the tower, described in later sections, the following two modifications were introduced in the line: 1- two water dual nozzles were installed facing downwards at the bottom end of the cylinder, and 2- a diversion of the slurry flow was put in place in the nozzle arm in Fig. 1, that feeds into an external storage tank.

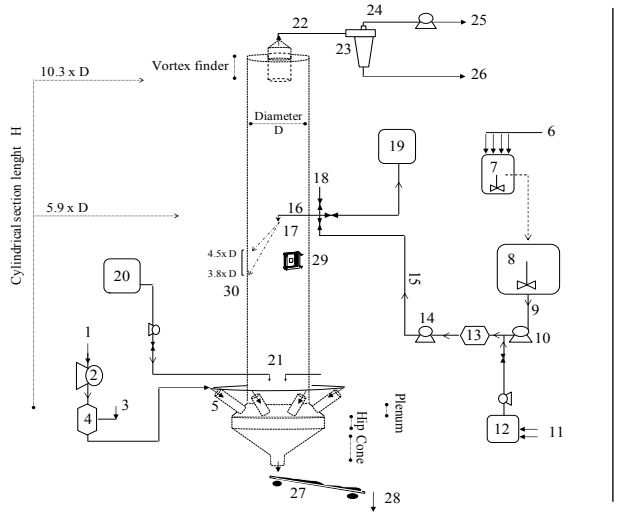

1- Ambient air feed
2- Hot air inlet air fan.
3- Fuel feed.
4- Burner.
5- Hot air inlet nozzle/s.
6- Slurry additions.
7- Crutcher. Batch.
8- Drop tank. Continuous.
9- Low pressure slurry line.
10- Low pressure pump.
11- Tracer and water feeds.
12- Storage. Tarcer solution.
13- Hammer mill. .
14- High pressure pump.
15- High pressure slurry line.
16- Nozzle arm.
17- Slurry pressure nozzle.
18- Purge. Air and vapour.
19- Slurry external storage.
20- Storage. Hot water.
21- Water dual nozzle/s.
22- Exhaust air line.
24- Exhaust air fan.
23- Cyclones.
26- Exit product. Cyclones.
25- Exhaust air outlet.
27- Tower belt.
28- Exit product. Tower belt.
29- Initial projection of the spray.
30- Inspection area monitored in Fig. 3.

Fig. 1. Outline of a counter-current spray drying tower, the operation of the slurry and air lines and the tracer injection system.

2.2 Outline of the tracer experiment.

The spray drying tower can be described in terms of two parallel systems, see Fig. 2a: 1- a hot air rising vortex that contains air-borne powder and 2- a separate structure comprised of particulate deposits that remains fixed at the wall. Both may be represented as distributed reactors where particles undergo different transformations. In the air-borne reactor particles dry, aggregate and flow, and in the wall-borne reactor, particles dry and may sinter but remain stationary. These two systems interact by rates of deposition and re-entrainment. This works identifies wall and air-borne populations experimentally. It focuses in quantifying the re-entrainment rate and the age of the granules involved in the deposition and re-entrainment cycle. A *"wash-out"* experiment is performed by executing a step change in the concentration of a tracer in the material fixed at the deposits. This allows evaluation of the release rate from the wall-borne reactor in Fig. 2a during a full renewal cycle, and the measurement of dye content as a function of particle size and exit time enabling calculation of the re-entrainment rate and the age of the re-entrained material.

This study requires generation of a set of traceable deposits such that at a given point the material borne at the walls contains the tracer while that in an air-borne state does not. Several stages, depicted in figure 2, are designed to achieve this, for a detailed description see [18]. The unit starts up under standard operation, which generates an initial stable layer of deposits, at this point untraceable, see Fig 2b. The dye injection is then connected, see Fig. 2c. To retain the tractability of the deposits generated thereafter, several precautions were taken:

- *Axial mixing:* After dye injection, the slurry flow is not diverted into the tower until it reaches the target, steady state, concentration at the nozzle level. Note that the axial mixing of the tracer in the line after injection could make the concentration at the nozzle to increase before stabilizing at the target value.

- *Wall deposits properties:* Special care also needs to be taken to ensure that the wall-borne structure in the tower is subject to similar air conditions at all times, particularly in relation to temperature, humidity and velocity, and thus that its moisture content and mechanical properties remain reasonably constant throughout the experiment.

For both of those purposes an intermediate stage is designed. When the tracer injection is connected in figure 2c, the slurry atomization stops, the slurry line is diverted towards an external storage tank and the nozzle arm section

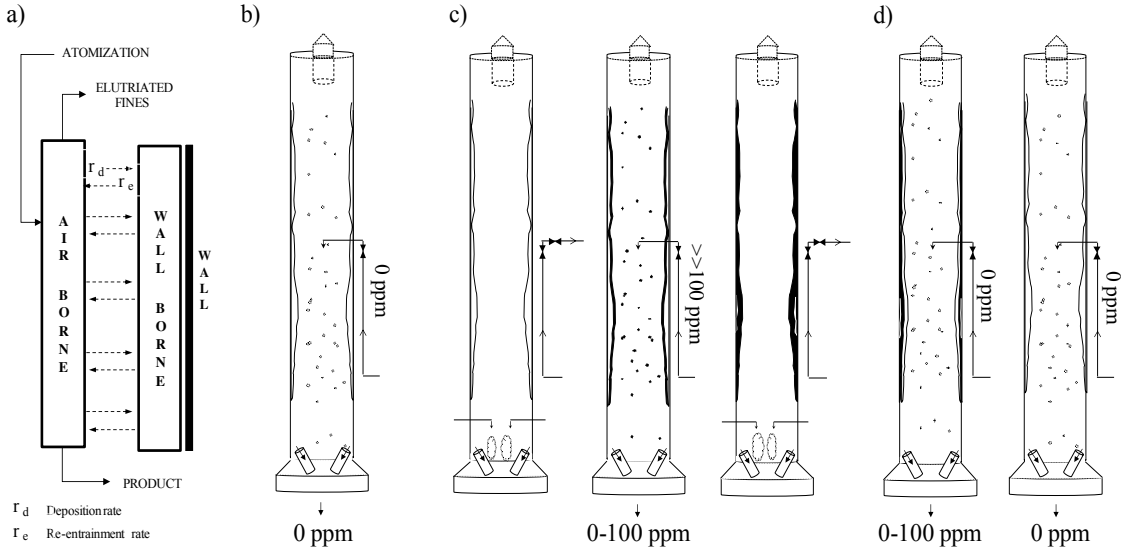

Fig. 2. (a) Counter-current spray driers as a combination of air-borne and wall-borne populations; (b) Initial standard operation with no tracer; (c) Operation with the tracer and associated intermediate stages; (d) Wash out of the traceable deposits under standard operation.

purged. The same operating conditions however can be maintained in the air line. This is achieved by atomizing pure water through dual nozzles at the bottom of the tower in the exact amount previously contained within the slurry flow. When the tracer achieves a constant concentration at the storage tank, the line is diverted back into the tower, atomization restarts and the water sprays are disconnected. All atomized droplets now contain a target dye concentration and any deposition and re-entrainment thereafter starts to generate layers of traceable material at the wall, see Fig. 2c. This renews the multi-layer until a new steady state is achieved and the entire active structure at the wall contains the dye. At this point the inverse sequence is executed for the disconnection of the injection. The slurry flow is diverted from the atomization to the external storage tank, what in effect empties the unit of all air-borne particles and leaves behind a set of traceable deposits at the walls. In the same manner, the connection of water sprays ensures that similar air conditions are maintained throughout the cylinder. When the slurry line is cleaned of any tracer the opposite changes are executed. Water sprays are disconnected, see the change from Fig. 2c to 2d, the slurry flow is diverted back into an empty tower, and thus when atomization restarts the droplets contain no tracer.

At that precise point the entire active structure fixed at the wall contains the tracer while the entire air-borne material does not. Hence, the rate of release of material from the walls may be quantified by measurement of the exit rate of the dye in a series of consecutive samples, differentiating the origin of aggregates from those coming from the atomizer, then white, or the wall-borne structure, dyed. A qualitative study of the re-entrainment mechanics can be made from observation of the distribution of dye within the granules. And, finally, the evolution of the release of dye permits one to estimate the average re-entrainment rate and the age time distribution of the re-entrained material.

3. Results and discussion.

3.1 A dynamic equilibrium

The evolution of the deposits is illustrated in Fig. 3a, by photographs of the inspection section depicted in Fig. 1, located in the area of projection of the atomization cone. Fig. 3b includes the weight evolution of the extractable plate during the time of execution of the experiment. At the initial stages, the weight of deposits increases at a constant rate, approximately 111 g min^{-1} m^{-2}. The weight then stabilizes and reaches a constant value after which no significant variations can be associated with any of the changes shown in Fig. 2; this indicates the deposits have similar properties and a constant overall weight during steady state operation, and thus net deposition rate is zero. Slight variations indicate detachment of small sections and are rather associated to the errors when removing and placing back the plate into position. However, looking at the transition in Fig. 3a to the production with tracer, as the atomized droplets start containing the dye an evident change follows in the color of deposits, which then reverses back again in the standard production at 7-8-9. As the weight of the deposits remains constant but droplet deposition occurs, the deposition of new material must be balanced by re-entrainment from the structure at the wall.

This observation demonstrates an active layer of deposits exists at the wall at least within the spray region, that is continuously renewed though the collisions of newly atomized droplets and the erosion of the wall-borne structure such as described in Fig. 2a. Consequently, a fraction of the tower product originates by the breakage of multi-layer structure, and its particle size and morphology, is rather related to the fouling dynamics and wall history rather than it is to the air-borne history. It is critical then to evaluate which proportion of the product is involved in this dynamics and how long it remains resident at the wall.

3.2 The equilibrium exchange rate

The dye content in pure dyed material, approximately 100 ppm, is obtained as a function of particle size by the analysis of the samples at the end of the production with the tracer, see Fig. 2c. This is the expected concentration in the powder should the air-borne and wall-borne material contain the dye. As product samples are taken when the multi-layer renews during the final standard production, see Fig. 2d, a proportion of the product appears as white containing no tracer, what corresponds to the material originated directly from the atomization. On the contrary, any

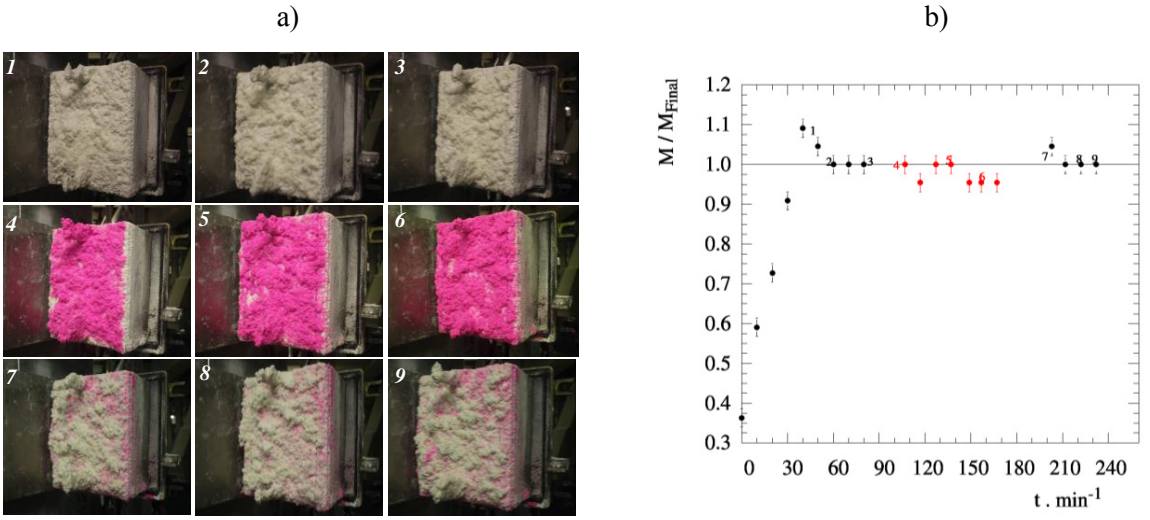

Fig. 3. (a) Inspection area within the spray projection for different production stages: 1-2-3 correspond to the initial standard production, see Fig. 2b, 4-5-6 and red color in (b) correspond to the production with tracer, see Fig. 2c. and 7-8-9 correspond to the wash out of traceable deposits see Fig. 2d.; (b) Evolution of the weight of the deposits in the inspection area (extractable plate plus deposits), for numbers and colors see (a).

dyed material has a single possible origin: the re-entrainment from the wall-borne structure. The ratio between the dye content of a mixture and that of the pure dyed powder at the same size range is denoted X, and defined below as a function of the sample absorbance, A, and dilution factor, S, for sampling time t and size ranges s. X corresponds to the ratio of dyed material in the mixture, what can be considered equivalent to the ratio of material in the sample that has a wall-borne origin.

$$X_{s,t} = \frac{S_{s,t} \cdot A_{s,t}}{S_{s,ref} \cdot A_{s,ref}} \tag{1}$$

The initial value of X can be taken as an estimation of the average re-entrainment rate, r_e , normalized by the production rate, M , that is : the proportion of the full production that is originated by re-entrainment. From the point atomization re-starts until the point where the tower is filled and has achieved the steady state rate, approximately 100 s, the mass averaged value of X decreases from an initial value of 20 ± 1 % to 12 ± 1 % of the rate. This range is in fact a conservative underestimation of the overall re-entrainment rate as the initial samples is an averaged value over the first 15 seconds of production- Hence, the actual re-entrainment rate could be in fact higher. It also varies substantially a function of size, increasing for both small and large fractions, up to 31 ± 2 % to 15 ± 1 % for the product below 212 µm, and up to a range between 37 ± 3 % to 10 ± 1 % for the fraction larger than 850 µm.

3.3 The wall-borne residence time.

As the active layer of the deposits renews the multi-layer starts containing white material given by the new deposited droplets. The re-entrained clusters start to be comprised of older dyed, plus younger white wall-borne material. This makes the value of X decrease until reaching zero when the structure is fully renewed (in this case becoming lower than 1 % after 3000 s). In a *"wash-out"* type of tracer experiment performed at a system of chemical reactors, analysis of the tracer release rate over a full renewal cycle determines the residence time distribution in the reactor. Similarly, analysis of the release rate of dye within the exit product in this case permits one to reconstruct the age probability density function of the re-entrained material, E, given below:

$$w_{s,i} = \frac{1}{2}\left(M_{s,i-1}X_{s,i-1} + M_{s,i}X_{s,i}\right) \quad (2)$$

$$W_s = \sum_{i=1}^{i=n-1} w_{s,i} \cdot \left(t_i - t_{1-1}\right) \quad (3)$$

$$E_{s,t} = \frac{w_{s,t}}{W_s} \quad (4)$$

In strict terms, E is not the residence time of the re-entrained material for this would also include a combination of the air-borne trajectories of the original primary droplets combined in the cluster, prior to their deposition. Here, E comprises of the wall-borne residence time of clusters and their air-borne trajectory from the re-entrainment event/s to the exit. E is estimated according to the exit rate of dyed material, w, given in (2) for a given size class s and time interval i between the i^{th} and i^{th}-1 samples, and normalized in (4) against the overall amount of dyed material that exits within a particular size class, denoted W_s and obtained from (3). Figure 4 compares the resulting normalized age distributions as a function of particle size. The entire set can be interpreted as the probability of the material borne at the wall to be re-entrained exiting at a given time t and within granules of a size class s. They all show a similar mode between 157.5 and 247.5 s, and an average first moment (average age) of 780 s, from 10 to 100 times above the residence time expected from the trajectories of mean particle sizes [19, 20]. This has important implications to the accepted view of counter-current spray driers, for it substantially increases the residence time of the product that undergoes deposition and re-entrainment and thus it affects its drying and growth history. With at least 12-20 % of particles going through the wall it is worth noting that these effects are likely to have a significant impact on the performance of numerical models of spray drying towers e.g. zonal models or computational fluid dynamics, CFD, models..

The age distribution itself varies significantly according to the granule size at which the re-entrained material exits. Two distinct set of functions are clearly visible in Fig. 4 according to whether to exit sizes are below or above 850 µm. In general terms, smaller and averaged size re-entrained particles exit the unit at a long time scale, what can be considered indicative of the diminishing concentration of dyed clusters in the multi-layer. Smaller sizes show

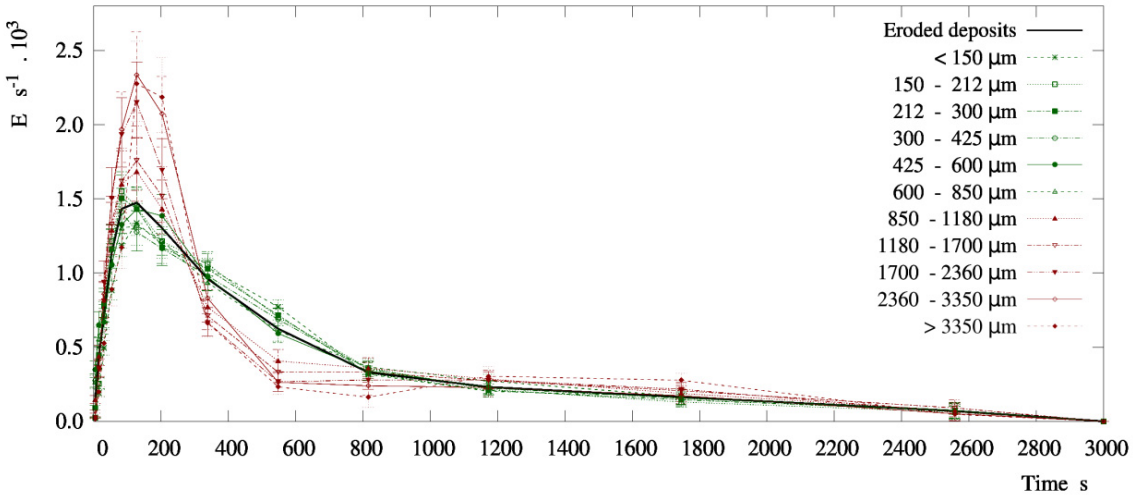

Fig. 4. Age probability density function of the re-entrained material, E. Comparison of the full product given in black, to the decomposition as a function of the exit size of the granule: direct re-entrainment of pure clusters from the deposits, given in green (typical of sizes < 850 µm) or wearing of aggregates of wall-borne clusters with air-borne material given in red (typical of sizes > 850 µm).

wide distributions and $t_{84\%}$ values ranging between 1350 s and 1560 s. On the contrary, as particle size increases > 850 µm, the granules exit at a much narrower time ranges. Age distributions progressively narrow around the mode as the size increases from 850 µm to values > 3000 µm, while they show higher $t_{84\%}$ values up to 1720 s. At least in regards to the development of the mode, it would appear that such narrow distributions rather than resulting from wall-borne residence time, are indicative of the continuous flow of large granules to the exit, and thus associated to a characteristic residence time, such as in a PFR reactor.

The air-borne residence time is in all cases far lower than the values derived from Fig. 4, and thus the differences observed must be caused by a different wall-borne residence times. This observation is supported by analysis of the structure of granules. Typical examples of the morphology for small and large particle size classes are given in Fig 5a and 5b respectively, obtained under optical microscopy. In general terms, smaller particles are re-entrained as pure dyed particles, undergoing no aggregation with air-borne material. However larger granules are eroded as mixtures and thus have been generated by the aggregation with droplets. This indicates that the different time scales observed in the age of re-entrained material are in fact correlated with different wear mechanics. Long time scales re-entrain small pure particles. This is likely caused by impacts of dry particles with sufficient inertia to break the structure but at a sufficiently dry state to prevent deposition or agglomeration. In parallel, a different re-entrainment mechanism involves the aggregation of air-borne and wall-borne material and dominates the formation of large granules which exit the unit faster and at a narrow time scale. This phenomenon is likely to be related to wall collisions of wet droplets at a high inertia. Coming directly from the atomization, such impacts may cause the capture of wall-borne clusters, and depending upon the impact momentum, can result in rolling, or a snowball type of effect (for a more detailed description of the contact mechanics and granules morphology see [18]).

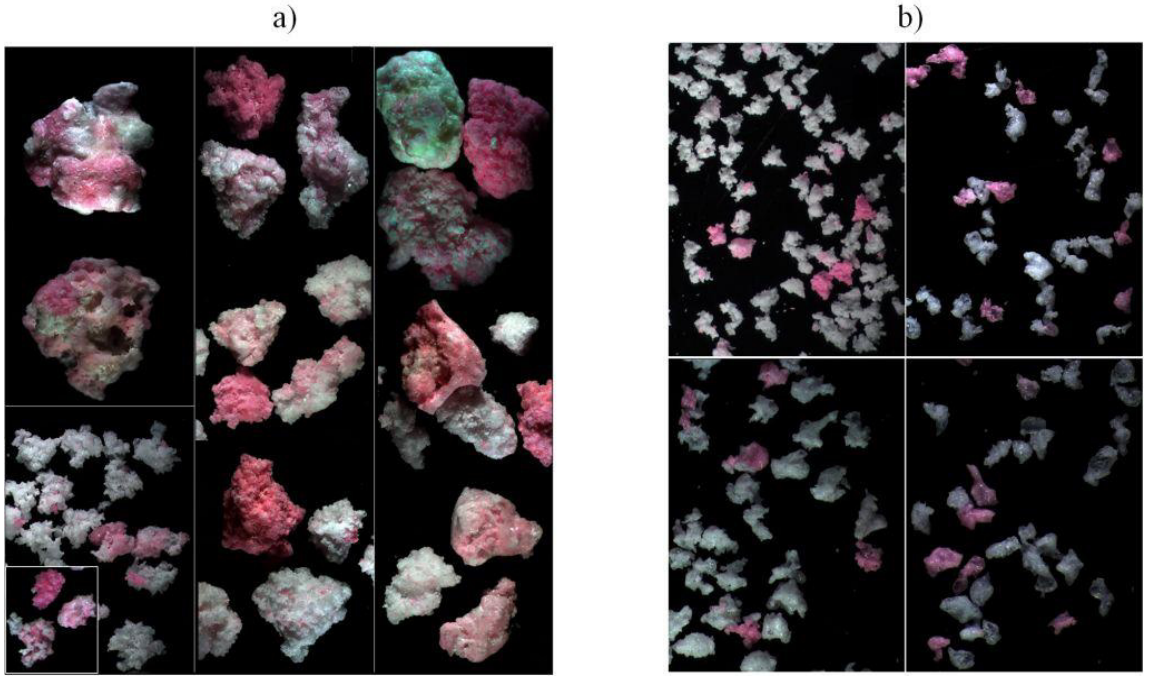

Fig. 5. Example of typical distributions of air and wall-borne material (a) mixtures in granules > 850 µm; (b) pure particles in smaller fractions.

Conclusions.

The work presented underscores the importance of fouling in counter-current spray driers, and the need to consider the interaction between material borne at the walls and the air-borne system. In the operation of a counter-

current spray drying tower manufacturing standard detergents, a dynamic equilibrium has been identified between the rates of deposition and re-entrainment, at least in the regions of highest deposition associated to the projection of the atomizing nozzles. The exchange rate of the deposition and re-entrainment cycle has been quantified in average terms at least between 12 to 20 % of the full production, which rises to 15 to 31 % for product smaller than 212 μm in diameter, or between 10 to 37 % for material larger than 850 μm.

Tracking of the rate of release of material from the walls has permitted quantification of the age distribution of the re-entrained powder. In average terms the age distribution shows a mode between 157.5 to 247.5 s, and a mean age of 780 s for this particular unit. These values are from 10 to 100 times above the expectation from the air-borne trajectories of particles, below 30 to 45 s for similar systems [19, 20]. Significant differences in the age of the re-entrained material appear as a function of the granule size at which it exits the unit, leading to the release of material from the walls at a large time scale release or a narrow age range should the re-entrained material exit in granules smaller or larger than approximately 850 μm. In parallel, similar size ranges in the product show clear differences in the way the re-entrained material distributes across individual granules, presenting either 1- pure particles in the case of smaller sizes or 2- mixtures of air and wall-borne material in granules > 850 μm. These observations suggest that different re-entrainment mechanisms are present in the process. Occurring at different time scales they cause either direct re-entrainment of clusters from the multi-layer, renewing gradually the structure, or aggregation between air and wall-borne material, generating large mixtures that roll down and exit in narrower time ranges.

In summary, the experimental evidence provided here demonstrates that the description of counter-current spray drying processes, in particular in regards to swirl assisted systems and detergent formulations necessitates recognition of the wall-borne state of particles. A better the description of the fouling process, the subsequent deposit's microstructure and its re-entrainment are considered critical steps ahead to improve the prediction of current numerical models in relation to both particle properties, and drying kinetics, and consequently process performance of a swirl spray dryer.

Acknowledgments.

VF was supported by an Engineering Doctorate Studentship sponsored by the Engineering and Physical Sciences Research Council (EPSRC) and Procter & Gamble in the Industrial Doctoral Centre in Formulation Engineering, School of Chemical Engineering, University of Birmingham.

The authors thank Mr. Andrew Roberts, Mr. Dave Banks and the crew at P&G in Newcastle upon Tyne for a very much appreciated involvement in this work.

Nomenclature

A	Absorbance.
D	Diameter of the cylindrical section of the spray dryer (m).
E	Age probability density function (s^{-1})
H	Length of the cylindrical section of the spray drying tower (m)
M	Mass rate (kg s^{-1}), or total weight of the extractable plate in Fig. 3 (kg)
S	Dilution factor (m^3 kg^{-1})
W	Mass exited in a given time and size range (kg).
X	Ratio of dyed material in the product, equivalent to the ratio of material of wall-borne origin. (-)
n	Number of samples.
r_e	Re-entrainment rate (kg s^{-1}).
r_d	Deposition rate (kg s^{-1}).
t	Time (s)
w	Exit rate of dyed or wall-borne material (kg s^{-1})

Subscripts

t	At time t, or in sample at time t.
ref	At the end of the production with the tracer injection connected, in Fig. 2c.
s	Size fraction

References

[1] Papavergos P.G. and Hedley, A.B. Particle deposition behaviour from turbulent flows. Chemical Engineering Research and Design, 62, 5, 275-295, 1984.

[2] Henry C., Minier J.P. and Lefevre G. Towards a description of particulate fouling: From single particle deposition to clogging. Advances incolloid and interface science, 185-186, 34-76, 2012.

[3] Wang H. and Harb J.N. Modeling of ash deposition in large-scale combustion facilities burning pulverized coal. Progress in energy and combustion science, 23, 267-282, 1997.

[4] Zbogar A., Frandsen F., Jensen P.A. and Glarborg P. Shedding of ash deposits. Progress in energy and combustion science, 35, 31-56, 2009.

[5] Liu L.X., Iveson S.M., Litster J.D. and Ennis. B.J. Coalescence of deformable granules in wet granulation processes. AIChE, 46, 529 -539, 2000.

[6] Kuschel M. and Sommerfeld M. Investigation of droplet collisions for solutions with different solids content. Experiments in Fluids, 54-1440, 2013.

[7] Verdurmen R.E.M., Menn P., Ritzert J., Blei S., Nhumaio G.C.S., Sørensen T.S., Gunsing M., Straatsma J., Verschueren M., Sibeijn M., Schulte G., Fritsching U., Bauckhage K., Tropea C., Sommerfeld M., Watkins, A.P., Yule A.J. and Schønfeldt H. Simulation of agglomeration in spray drying installations: The EDECAD project. Drying technology, 22, 6, 1403-1461, 2004.

[8] Hoeven M.J. Particle - Droplet collisions in spray drying. Ph.D. dissertation. School of Engineering. University of Queensland, 2008.

[9] Focke C., Kuschel M., Sommerfeld M. and Bothe D.. Collision between high and low viscosity droplets: Direct Numerical Simulations and experiments. International journal of multiphase flow, 56, 81-92, 2013.

[10] Ozmen L. and Langrish T.A.G. An experimental investigation of the wall deposition of milk powder in a pilot-scale spray dryer. Drying technology, 21, 7, 1235–1252, 2003.

[11] Kota K. and Langrish T. A. G. Fluxes and patterns of wall deposits for skim milk in a pilot-scale spray dryer. Drying technology, 24, 8, 993-1001, 2006.

[12] Langrish T.A. and Zbiciński I. The effects of air inlet geometry and spray cone angle on the wall deposition rate in spray dryers. Chemical engineering research and design. 72, A3, 420-430, 1994.

[13] Hanus M.J. and Langrish T.A.G. Re-entrainment of wall deposits from a laboratory-scale spray dryer. Asia-Pac. Journal of chemical engineering, 2, 90-107, 2007a.

[14] Kota K., and Langrish T.A.G. Prediciton of wall deposition behaviour in a pilot-scale spray dryer using deposition correlations for pipe flows. Journal of Zhejiang University Science A, 8, 301–312, 2007.

[15] Hanus M.J. and Langrish T.A.G. Resuspension of wall deposits in spray dryers. J. Zhejiang University Science A., 8, 11, 1762-1774, 2007b.

[16] Huntington D. H. The influence of the spray drying process on product properties. Drying technology, 22, 6, 1261-1287, 2004.

[17] Hassall G. Wall build up in spray driers. EngD dissertation. Chemical Engineering. University of Birmingham, 2011.

[18] Francia, V., Martin, L., Bayly, A.E. and Simmons, M.J.H. Experimental evidence of the role of wall deposition and re-entrainment within a swirl counter-current spray drying tower. AIChE. To be submitted, 2014.

[19] Ali M., Mahmud T., Heggs P.J., Ghadiri M., Francia V., Bayly A.E., Djurdjevic D., Ahmadian H. and Martin L. CFD modeling of a counter-current spray drying tower. International conference in multiphase flow. Jeju, South Korea, 2013.

[20] Harvie D.J.E., Langrish T.A.G. and Fletcher D.F. A computational fluid dynamics study of a tall-form spray dryer. Trans IChemE, 80, Part C, 163 – 175, 2002.